Supplement of Earth Syst. Dynam., 14, 1363–1374, 2023
https://doi.org/10.5194/esd-14-1363-2023-supplement

Earth System Dynamics
Open Access

Supplement of

Understanding variations in downwelling longwave radiation using Brutsaert's equation

Yinglin Tian et al.

Correspondence to: Axel Kleidon (akleidon@bgc-jena.mpg.de)

Table S1. FLUXNET stations used in this study, including their FLUXNET ID, latitude, longitude, the years used in the analysis, and the doi reference to the site.

No.	FLUXNETID	Lat	Lon	Begin Year	End Year	DOI
1	AR-SLu	-33.46	-66.46	2009	2011	https://doi.org/10.18140/flx/1440191
2	AR-Vir	-28.24	-56.19	2009	2012	https://doi.org/10.18140/flx/1440192
3	AT-Neu	47.12	11.32	2002	2012	https://doi.org/10.18140/flx/1440121
4	AU-Ade	-13.08	131.12	2007	2009	https://doi.org/10.18140/flx/1440193
5	AU-ASM	-22.28	133.25	2010	2014	https://doi.org/10.18140/flx/1440194
6	AU-Cpr	-34.00	140.59	2010	2014	https://doi.org/10.18140/flx/1440195
7	AU-Cum	-33.61	150.72	2012	2014	https://doi.org/10.18140/flx/1440196
8	AU-DaP	-14.06	131.32	2007	2013	https://doi.org/10.18140/flx/1440123
9	AU-DaS	-14.16	131.39	2008	2014	https://doi.org/10.18140/flx/1440122
10	AU-Dry	-15.26	132.37	2008	2014	https://doi.org/10.18140/flx/1440197
11	AU-Emr	-23.86	148.47	2011	2013	https://doi.org/10.18140/flx/1440198
12	AU-Fog	-12.55	131.31	2006	2008	https://doi.org/10.18140/flx/1440124
13	AU-Gin	-31.38	115.71	2011	2014	https://doi.org/10.18140/flx/1440199
14	AU-GWW	-30.19	120.65	2013	2014	https://doi.org/10.18140/flx/1440200
15	AU-How	-12.49	131.15	2001	2014	https://doi.org/10.18140/flx/1440125
16	AU-Lox	-34.47	140.66	2008	2009	https://doi.org/10.18140/flx/1440247
17	AU-RDF	-14.56	132.48	2011	2013	https://doi.org/10.18140/flx/1440201
18	AU-Rig	-36.65	145.58	2011	2014	https://doi.org/10.18140/flx/1440202
19	AU-Rob	-17.12	145.63	2014	2014	https://doi.org/10.18140/flx/1440203
20	AU-Stp	-17.15	133.35	2008	2014	https://doi.org/10.18140/flx/1440204
21	AU-TTE	-22.29	133.64	2012	2014	https://doi.org/10.18140/flx/1440205
22	AU-Tum	-35.66	148.15	2001	2014	https://doi.org/10.18140/flx/1440126
23	AU-Wac	-37.43	145.19	2005	2008	https://doi.org/10.18140/flx/1440127
24	AU-Whr	-36.67	145.03	2011	2014	https://doi.org/10.18140/flx/1440206
25	AU-Wom	-37.42	144.09	2010	2014	https://doi.org/10.18140/flx/1440207
26	AU-Ync	-34.99	146.29	2012	2014	https://doi.org/10.18140/flx/1440208
27	BE-Bra	51.31	4.52	1996	2014	https://doi.org/10.18140/flx/1440128
28	BE-Lon	50.55	4.75	2004	2014	https://doi.org/10.18140/flx/1440129
29	BE-Vie	50.31	6.00	1996	2014	https://doi.org/10.18140/flx/1440130
30	BR-Sa1	-2.86	-54.96	2002	2011	https://doi.org/10.18140/flx/1440032
31	BR-Sa3	-3.02	-54.97	2000	2004	https://doi.org/10.18140/flx/1440033
32	CA-Gro	48.22	-82.16	2003	2014	https://doi.org/10.18140/flx/1440034
33	CA-Man	55.88	-98.48	1994	2008	https://doi.org/10.18140/flx/1440035
34	CA-NS1	55.88	-98.48	2001	2005	https://doi.org/10.18140/flx/1440036
35	CA-NS2	55.91	-98.52	2001	2005	https://doi.org/10.18140/flx/1440037
36	CA-NS3	55.91	-98.38	2001	2005	https://doi.org/10.18140/flx/1440038
37	CA-NS4	55.91	-98.38	2002	2005	https://doi.org/10.18140/flx/1440039
38	CA-NS5	55.86	-98.49	2001	2005	https://doi.org/10.18140/flx/1440040
39	CA-NS6	55.92	-98.96	2001	2005	https://doi.org/10.18140/flx/1440041
40	CA-NS7	56.64	-99.95	2002	2005	https://doi.org/10.18140/flx/1440042
41	CA-Oas	53.63	-106.20	1996	2010	https://doi.org/10.18140/flx/1440043
42	CA-Obs	53.99	-105.12	1997	2010	https://doi.org/10.18140/flx/1440044
43	CA-Qfo	49.69	-74.34	2003	2010	https://doi.org/10.18140/flx/1440045
44	CA-SF1	54.49	-105.82	2003	2006	https://doi.org/10.18140/flx/1440046
45	CA-SF2	54.25	-105.88	2001	2005	https://doi.org/10.18140/flx/1440047
46	CA-SF3	54.09	-106.01	2001	2006	https://doi.org/10.18140/flx/1440048

No.	FLUXNETID	Lat	Lon	BegionYear	EndYear	DOI
47	CA-TP1	42.66	-80.56	2002	2014	https://doi.org/10.18140/flx/1440050
48	CA-TP2	42.77	-80.46	2002	2007	https://doi.org/10.18140/flx/1440051
49	CA-TP3	42.71	-80.35	2002	2014	https://doi.org/10.18140/flx/1440052
50	CA-TP4	42.71	-80.36	2002	2014	https://doi.org/10.18140/flx/1440053
51	CA-TPD	42.64	-80.56	2012	2014	https://doi.org/10.18140/flx/1440112
52	CG-Tch	-4.29	11.66	2006	2009	https://doi.org/10.18140/flx/1440142
53	CH-Cha	47.21	8.41	2005	2014	https://doi.org/10.18140/flx/1440131
54	CH-Dav	46.82	9.86	1997	2014	https://doi.org/10.18140/flx/1440132
55	CH-Fru	47.12	8.54	2005	2014	https://doi.org/10.18140/flx/1440133
56	CH-Lae	47.48	8.37	2004	2014	https://doi.org/10.18140/flx/1440134
57	CH-Oe1	47.29	7.73	2002	2008	https://doi.org/10.18140/flx/1440135
58	CH-Oe2	47.29	7.73	2004	2014	https://doi.org/10.18140/flx/1440136
59	CN-Cha	42.40	128.10	2003	2005	https://doi.org/10.18140/flx/1440137
60	CN-Cng	44.59	123.51	2007	2010	https://doi.org/10.18140/flx/1440209
61	CN-Dan	30.50	91.07	2004	2005	https://doi.org/10.18140/flx/1440138
62	CN-Din	23.17	112.54	2003	2005	https://doi.org/10.18140/flx/1440139
63	CN-Du2	42.05	116.28	2006	2008	https://doi.org/10.18140/flx/1440140
64	CN-Du3	42.06	116.28	2009	2010	https://doi.org/10.18140/flx/1440210
65	CN-Ha2	37.61	101.33	2003	2005	https://doi.org/10.18140/flx/1440211
66	CN-HaM	37.37	101.18	2002	2004	https://doi.org/10.18140/flx/1440190
67	CN-Qia	26.74	115.06	2003	2005	https://doi.org/10.18140/flx/1440141
68	CN-Sw2	41.79	111.90	2010	2012	https://doi.org/10.18140/flx/1440212
69	CZ-BK1	49.50	18.54	2004	2014	https://doi.org/10.18140/flx/1440143
70	CZ-BK2	49.49	18.54	2004	2012	https://doi.org/10.18140/flx/1440144
71	CZ-wet	49.02	14.77	2006	2014	https://doi.org/10.18140/flx/1440145
72	DE-Akm	53.87	13.68	2009	2014	https://doi.org/10.18140/flx/1440213
73	DE-Geb	51.10	10.91	2001	2014	https://doi.org/10.18140/flx/1440146
74	DE-Gri	50.95	13.51	2004	2014	https://doi.org/10.18140/flx/1440147
75	DE-Hai	51.08	10.45	2000	2012	https://doi.org/10.18140/flx/1440148
76	DE-Kli	50.89	13.52	2004	2014	https://doi.org/10.18140/flx/1440149
77	DE-Lkb	49.10	13.30	2009	2013	https://doi.org/10.18140/flx/1440214
78	DE-Lnf	51.33	10.37	2002	2012	https://doi.org/10.18140/flx/1440150
79	DE-Obe	50.78	13.72	2008	2014	https://doi.org/10.18140/flx/1440151
80	DE-RuR	50.62	6.30	2011	2014	https://doi.org/10.18140/flx/1440215
81	DE-RuS	50.87	6.45	2011	2014	https://doi.org/10.18140/flx/1440216
82	DE-Seh	50.87	6.45	2007	2010	https://doi.org/10.18140/flx/1440217
83	DE-SfN	47.81	11.33	2012	2014	https://doi.org/10.18140/flx/1440219
84	DE-Spw	51.89	14.03	2010	2014	https://doi.org/10.18140/flx/1440220
85	DE-Tha	50.96	13.57	1996	2014	https://doi.org/10.18140/flx/1440152
86	DE-Zrk	53.88	12.89	2013	2014	https://doi.org/10.18140/flx/1440221
87	DK-Eng	55.69	12.19	2005	2008	https://doi.org/10.18140/flx/1440153
88	DK-Fou	56.48	9.59	2005	2005	https://doi.org/10.18140/flx/1440154
89	DK-Sor	55.49	11.64	1996	2014	https://doi.org/10.18140/flx/1440155
90	ES-Amo	36.83	-2.25	2007	2012	https://doi.org/10.18140/flx/1440156
91	ES-LgS	37.10	-2.97	2007	2009	https://doi.org/10.18140/flx/1440225
92	ES-LJu	36.93	-2.75	2004	2013	https://doi.org/10.18140/flx/1440157
93	ES-Ln2	36.97	-3.48	2009	2009	https://doi.org/10.18140/flx/1440226
94	FI-Hyy	61.85	24.30	1996	2014	https://doi.org/10.18140/flx/1440158
95	FI-Jok	60.90	23.51	2000	2003	https://doi.org/10.18140/flx/1440159
96	FI-Let	60.64	23.96	2009	2012	https://doi.org/10.18140/flx/1440227

No.	FLUXNETID	Lat	Lon	BegionYear	EndYear	DOI
97	FI-Lom	68.00	24.21	2007	2009	https://doi.org/10.18140/flx/1440228
98	FI-Sod	67.36	26.64	2001	2014	https://doi.org/10.18140/flx/1440160
99	FR-Fon	48.48	2.78	2005	2014	https://doi.org/10.18140/flx/1440161
100	FR-Gri	48.84	1.95	2004	2014	https://doi.org/10.18140/flx/1440162
101	FR-LBr	44.72	-0.77	1996	2008	https://doi.org/10.18140/flx/1440163
102	FR-Pue	43.74	3.60	2000	2014	https://doi.org/10.18140/flx/1440164
103	GF-Guy	5.28	-52.92	2004	2014	https://doi.org/10.18140/flx/1440165
104	GH-Ank	5.27	-2.69	2011	2014	https://doi.org/10.18140/flx/1440229
105	IT-BCi	40.52	14.96	2004	2014	https://doi.org/10.18140/flx/1440166
106	IT-CA1	42.38	12.03	2011	2014	https://doi.org/10.18140/flx/1440230
107	IT-CA2	42.38	12.03	2011	2014	https://doi.org/10.18140/flx/1440231
108	IT-CA3	42.38	12.02	2011	2014	https://doi.org/10.18140/flx/1440232
109	IT-Col	41.85	13.59	1996	2014	https://doi.org/10.18140/flx/1440167
110	IT-Cp2	41.70	12.36	2012	2014	https://doi.org/10.18140/flx/1440233
111	IT-Cpz	41.71	12.38	1997	2009	https://doi.org/10.18140/flx/1440168
112	IT-Isp	45.81	8.63	2013	2014	https://doi.org/10.18140/flx/1440234
113	IT-La2	45.95	11.29	2000	2002	https://doi.org/10.18140/flx/1440235
114	IT-Lav	45.96	11.28	2003	2014	https://doi.org/10.18140/flx/1440169
115	IT-MBo	46.01	11.05	2003	2013	https://doi.org/10.18140/flx/1440170
116	IT-Noe	40.61	8.15	2004	2014	https://doi.org/10.18140/flx/1440171
117	IT-PT1	45.20	9.06	2002	2004	https://doi.org/10.18140/flx/1440172
118	IT-Ren	46.59	11.43	1998	2013	https://doi.org/10.18140/flx/1440173
119	IT-Ro1	42.41	11.93	2000	2008	https://doi.org/10.18140/flx/1440174
120	IT-Ro2	42.39	11.92	2002	2012	https://doi.org/10.18140/flx/1440175
121	IT-SR2	43.73	10.29	2013	2014	https://doi.org/10.18140/flx/1440236
122	IT-SRo	43.73	10.28	1999	2012	https://doi.org/10.18140/flx/1440176
123	IT-Tor	45.84	7.58	2008	2014	https://doi.org/10.18140/flx/1440237
124	JP-MBF	44.39	142.32	2003	2005	https://doi.org/10.18140/flx/1440238
125	JP-SMF	35.26	137.08	2002	2006	https://doi.org/10.18140/flx/1440239
126	MY-PSO	2.97	102.31	2003	2009	https://doi.org/10.18140/flx/1440240
127	NL-Hor	52.24	5.07	2004	2011	https://doi.org/10.18140/flx/1440177
128	NL-Loo	52.17	5.74	1996	2014	https://doi.org/10.18140/flx/1440178
129	PA-SPs	9.31	-79.63	2007	2009	https://doi.org/10.18140/flx/1440179
130	RU-Che	68.61	161.34	2002	2005	https://doi.org/10.18140/flx/1440181
131	RU-Cok	70.83	147.49	2003	2014	https://doi.org/10.18140/flx/1440182
132	RU-Fyo	56.46	32.92	1998	2014	https://doi.org/10.18140/flx/1440183
133	RU-Ha1	54.73	90.00	2002	2004	https://doi.org/10.18140/flx/1440184
134	SD-Dem	13.28	30.48	2005	2009	https://doi.org/10.18140/flx/1440186
135	SN-Dhr	15.40	-15.43	2010	2013	https://doi.org/10.18140/flx/1440246
136	US-AR1	36.43	-99.42	2009	2012	https://doi.org/10.18140/flx/1440103
137	US-AR2	36.64	-99.60	2009	2012	https://doi.org/10.18140/flx/1440104
138	US-ARb	35.55	-98.04	2005	2006	https://doi.org/10.18140/flx/1440064
139	US-ARc	35.55	-98.04	2005	2006	https://doi.org/10.18140/flx/1440065
140	US-ARM	36.61	-97.49	2003	2012	https://doi.org/10.18140/flx/1440066
141	US-Atq	70.47	-157.41	2003	2008	https://doi.org/10.18140/flx/1440067
142	US-Blo	38.90	-120.63	1997	2007	https://doi.org/10.18140/flx/1440068
143	US-Cop	38.09	-109.39	2001	2007	https://doi.org/10.18140/flx/1440100
144	US-CRT	41.63	-83.35	2011	2013	https://doi.org/10.18140/flx/1440117
145	US-GBT	41.37	-106.24	1999	2006	https://doi.org/10.18140/flx/1440118
146	US-GLE	41.37	-106.24	2004	2014	https://doi.org/10.18140/flx/1440069

No.	FLUXNETID	Lat	Lon	BegionYear	EndYear	DOI
147	US-Goo	34.25	-89.87	2002	2006	https://doi.org/10.18140/flx/1440070
148	US-Ha1	42.54	-72.17	1991	2012	https://doi.org/10.18140/flx/1440071
149	US-IB2	41.84	-88.24	2004	2011	https://doi.org/10.18140/flx/1440072
150	US-Ivo	68.49	-155.75	2004	2007	https://doi.org/10.18140/flx/1440073
151	US-KS1	28.46	-80.67	2002	2002	https://doi.org/10.18140/flx/1440074
152	US-KS2	28.61	-80.67	2003	2006	https://doi.org/10.18140/flx/1440075
153	US-Lin	36.36	-119.84	2009	2010	https://doi.org/10.18140/flx/1440107
154	US-Los	46.08	-89.98	2000	2014	https://doi.org/10.18140/flx/1440076
155	US-LWW	34.96	-97.98	1997	1998	https://doi.org/10.18140/flx/1440077
156	US-Me1	44.58	-121.50	2004	2005	https://doi.org/10.18140/flx/1440078
157	US-Me2	44.45	-121.56	2002	2014	https://doi.org/10.18140/flx/1440079
158	US-Me3	44.32	-121.61	2004	2009	https://doi.org/10.18140/flx/1440080
159	US-Me4	44.50	-121.62	1996	2000	https://doi.org/10.18140/flx/1440081
160	US-Me5	44.44	-121.57	2000	2002	https://doi.org/10.18140/flx/1440082
161	US-Me6	44.32	-121.61	2010	2014	https://doi.org/10.18140/flx/1440099
162	US-MMS	39.32	-86.41	1999	2014	https://doi.org/10.18140/flx/1440083
163	US-Myb	38.05	-121.77	2010	2014	https://doi.org/10.18140/flx/1440105
164	US-Ne1	41.17	-96.48	2001	2013	https://doi.org/10.18140/flx/1440084
165	US-Ne2	41.16	-96.47	2001	2013	https://doi.org/10.18140/flx/1440085
166s	US-Ne3	41.18	-96.44	2001	2013	https://doi.org/10.18140/flx/1440086
167	US-NR1	40.03	-105.55	1998	2014	https://doi.org/10.18140/flx/1440087
168	US-Oho	41.55	-83.84	2004	2013	https://doi.org/10.18140/flx/1440088
169	US-ORv	40.02	-83.02	2011	2011	https://doi.org/10.18140/flx/1440102
170s	US-PFa	45.95	-90.27	1995	2014	https://doi.org/10.18140/flx/1440089
171	US-Prr	65.12	-147.49	2010	2014	https://doi.org/10.18140/flx/1440113
172	US-SRC	31.91	-110.84	2008	2014	https://doi.org/10.18140/flx/1440098
173	US-SRG	31.79	-110.83	2008	2014	https://doi.org/10.18140/flx/1440114
174	US-SRM	31.82	-110.87	2004	2014	https://doi.org/10.18140/flx/1440090
175	US-Sta	41.40	-106.80	2005	2009	https://doi.org/10.18140/flx/1440115
176	US-Syv	46.24	-89.35	2001	2014	https://doi.org/10.18140/flx/1440091
177	US-Ton	38.43	-120.97	2001	2014	https://doi.org/10.18140/flx/1440092
178	US-Tw1	38.11	-121.65	2012	2014	https://doi.org/10.18140/flx/1440108
179	US-Tw2	38.10	-121.64	2012	2013	https://doi.org/10.18140/flx/1440109
180	US-Tw3	38.12	-121.65	2013	2014	https://doi.org/10.18140/flx/1440110
181	US-Tw4	38.10	-121.64	2013	2014	https://doi.org/10.18140/flx/1440111
182	US-Twt	38.11	-121.65	2009	2014	https://doi.org/10.18140/flx/1440106
183	US-UMB	45.56	-84.71	2000	2014	https://doi.org/10.18140/flx/1440093
184	US-UMd	45.56	-84.70	2007	2014	https://doi.org/10.18140/flx/1440101
185	US-Var	38.41	-120.95	2000	2014	https://doi.org/10.18140/flx/1440094
186	US-WCr	45.81	-90.08	1999	2014	https://doi.org/10.18140/flx/1440095
187	US-Whs	31.74	-110.05	2007	2014	https://doi.org/10.18140/flx/1440097
188	US-Wi0	46.62	-91.08	2002	2002	https://doi.org/10.18140/flx/1440055
189	US-Wi1	46.73	-91.23	2003	2003	https://doi.org/10.18140/flx/1440054

Table S2. Statistics of the number of data points of different variables with different quality controls in the FLUXNET dataset.

Data amount	R_{ld}	R_s	e_a	T_a
All data	14587695	24424933	23353543	24200040
Data with quality control as 0, 1 or 2	13264714	22870933	21571808	22736876
Data with quality control as 0	12759714	22386602	20646599	22060360

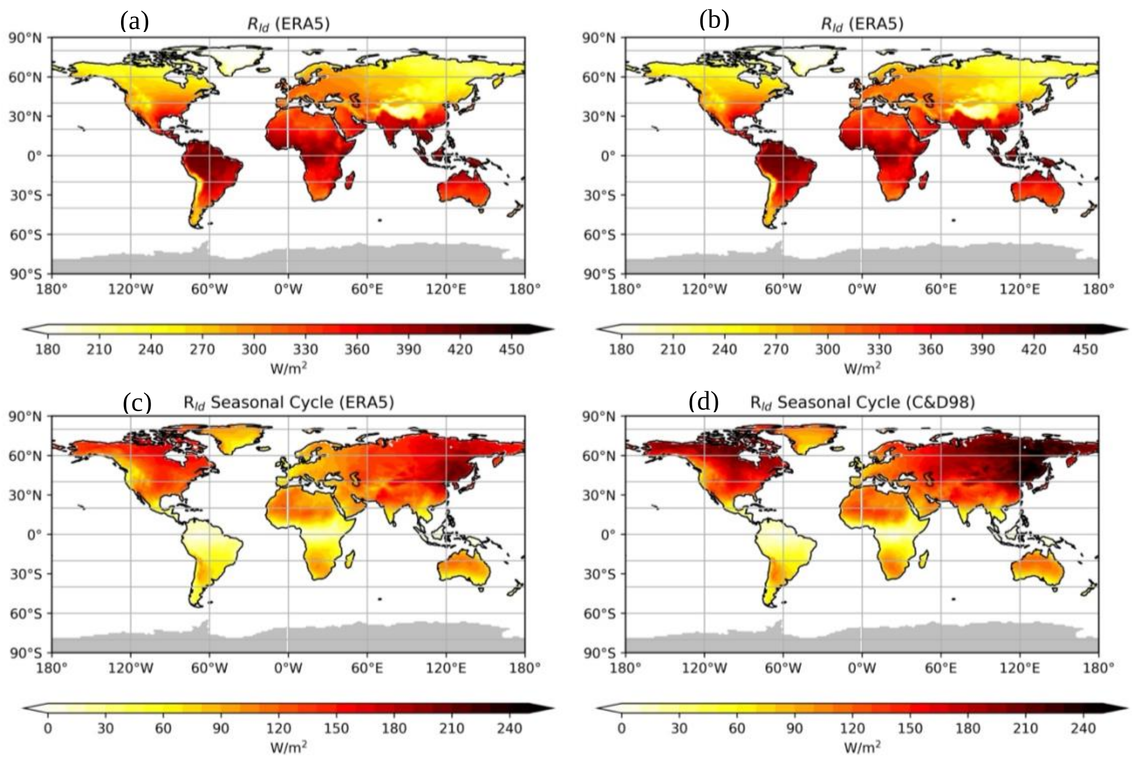

Figure S1. The same as Fig. 1 but for ERA5 dataset.

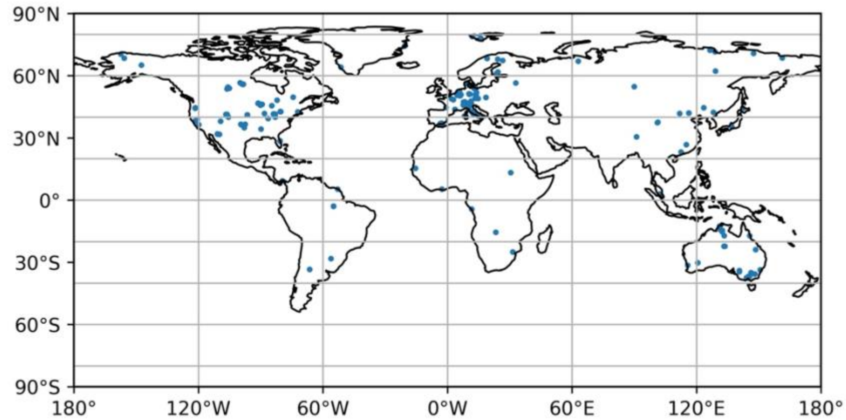

Figure S2. Locations of the 189 FLUXNET sites used in the study.

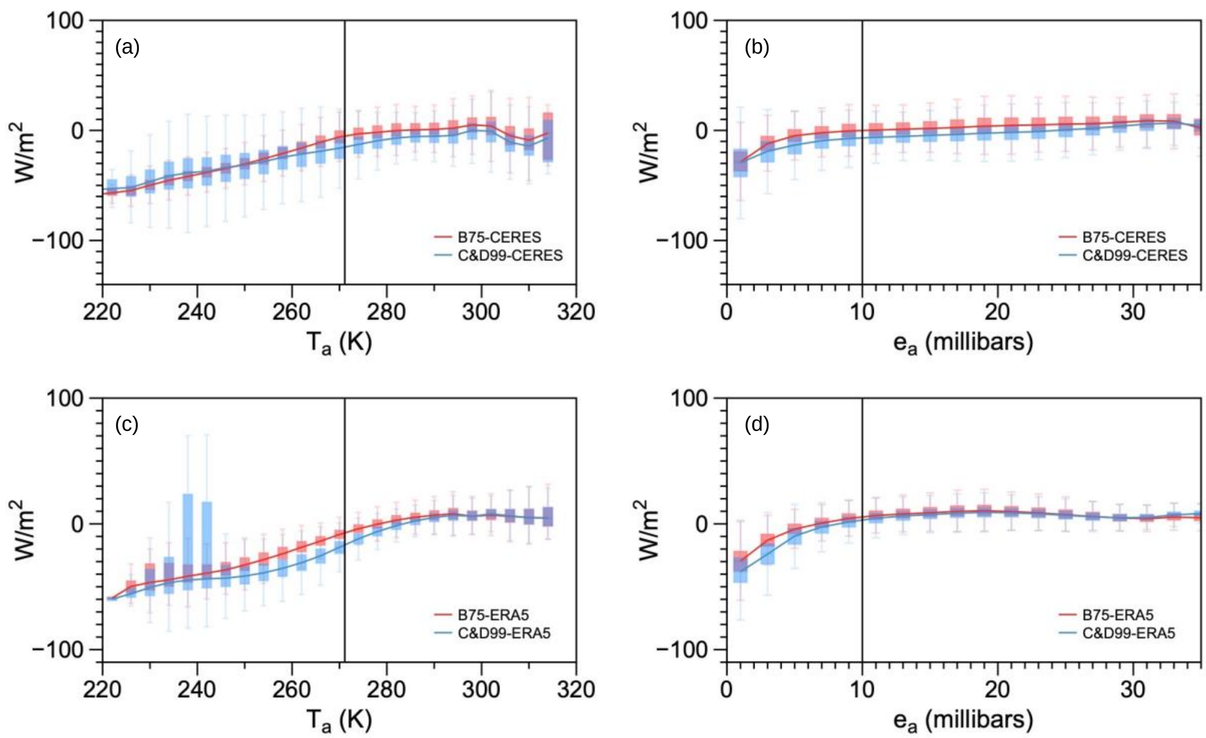

Figure S3. The same as Figs. 3a and 3b but with data from (a and c) ERA5 and (b and d) CERES data.

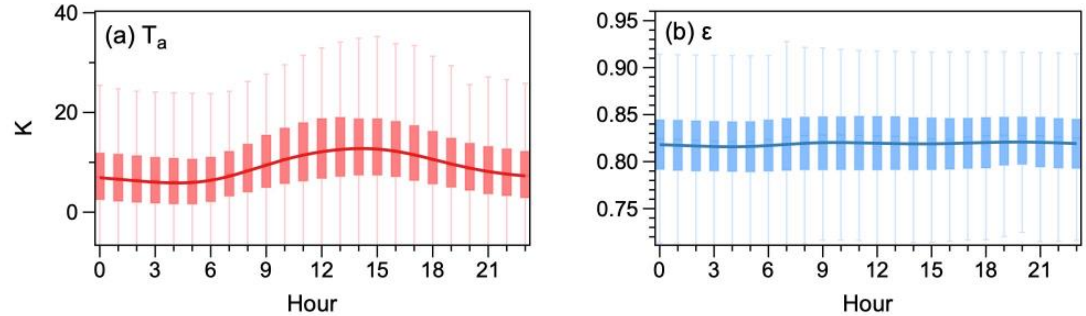

Figure S4. The multi-year mean diurnal variations in (a) T_a and (b) water vapor pressure in the FLUXNET dataset aggregated over 189 sites. The box shows the variation among the 189 FLUXNET sites. The upper and lower whiskers indicate 95^{th} and 5^{th} percentiles, upper boundary, median line, and lower boundary of the box indicate the 75^{th}, 50^{th}, 25^{th} quantiles, respectively. The solid lines are Loess fit.

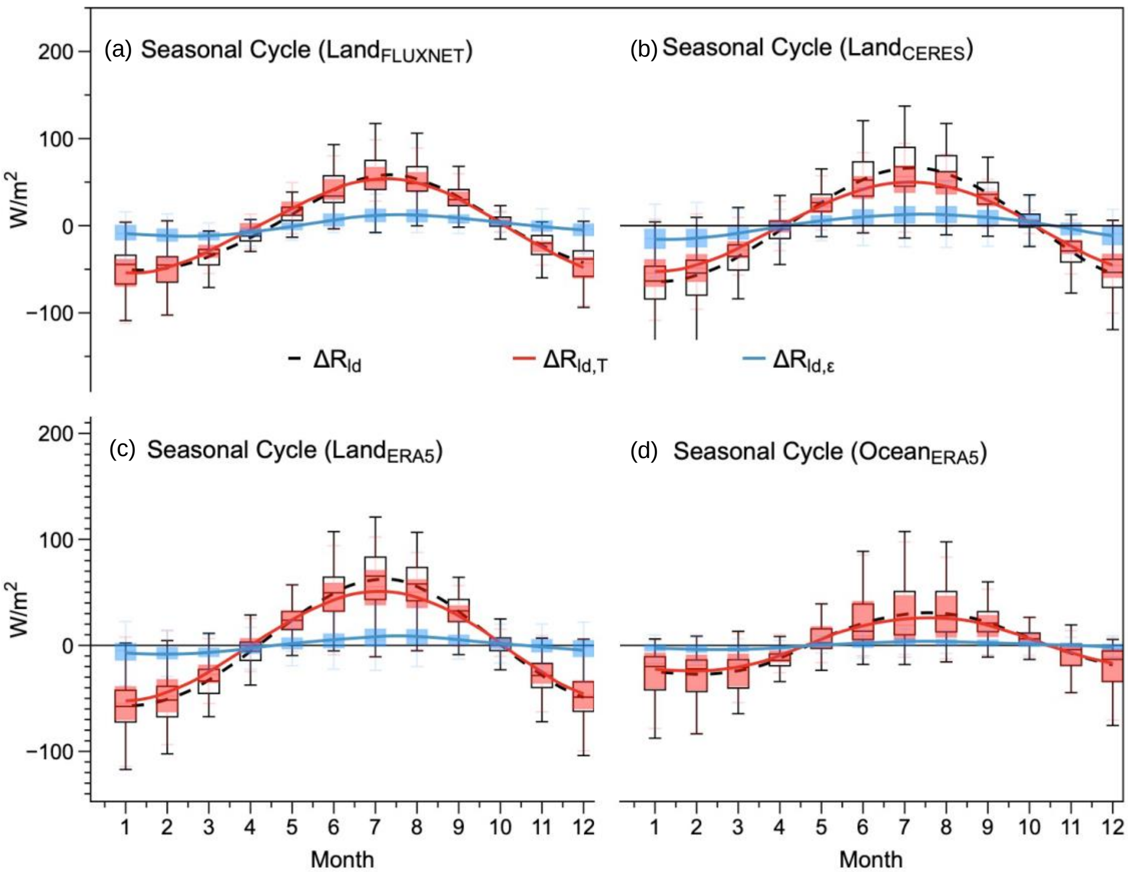

Figure S5. Seasonal cycle of R_{ld} and their decomposition into the contribution of changes in emissivity and low-level atmospheric heat storage based on (a, b) FUXNET site data, and (c, d) ERA5 monthly grid data (a, b, c) over land and (d) ocean. The box shows the variation among the grids/sites. The upper and lower whiskers indicate 95^{th} and 5^{th} percentiles, upper boundary, median line, and lower boundary of the box indicate the 75^{th}, 50^{th}, 25^{th} quantiles, respectively. The solid/dash lines are Loess fit. For each site/grid and each month, the multiyear-mean value is removed, and thus the deviations are shown.

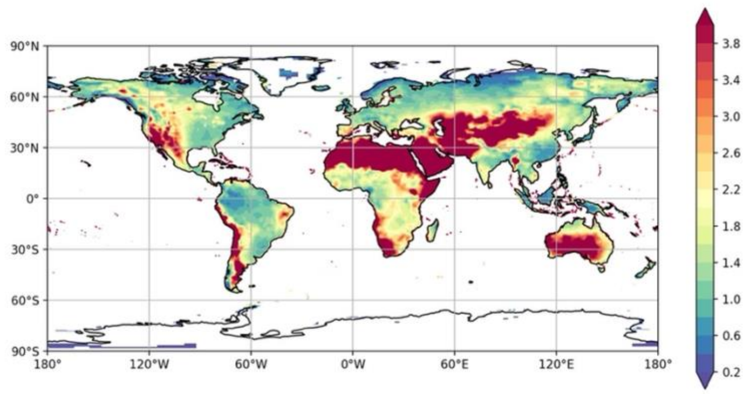

Fig. S6 Distribution of the aridity over land. Data is from NASA-CERES.

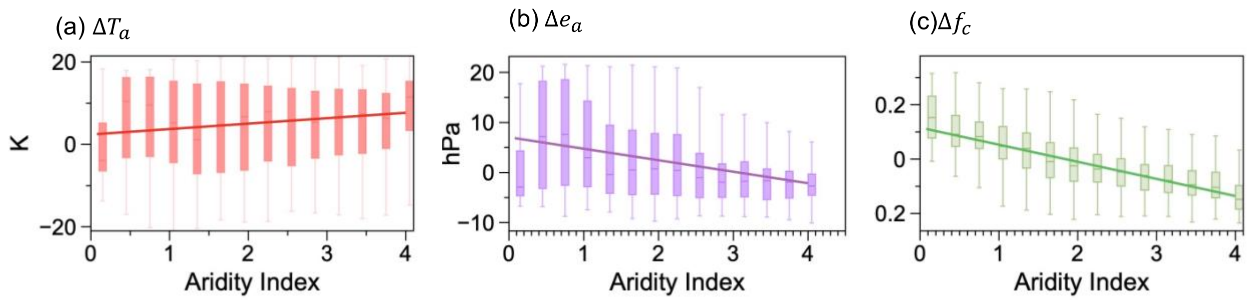

Figure S7. Variations along with aridity index of multiyear-mean (a) surface temperature, (b) water vapor pressure, and (c) cloud cover. The box shows the variation among the land grids with the same aridity index, while the solid line is the linear regression. The upper and lower whisker indicate 95th and 5th percentiles, upper boundary, median line, and lower boundary of the box indicate the 75th, 50th, 25th quantiles, respectively. For each grid, the multiyear-mean land-average value is extracted, and thus the spatial deviations (Δ) are shown. Data are from the NASA-CERES dataset.

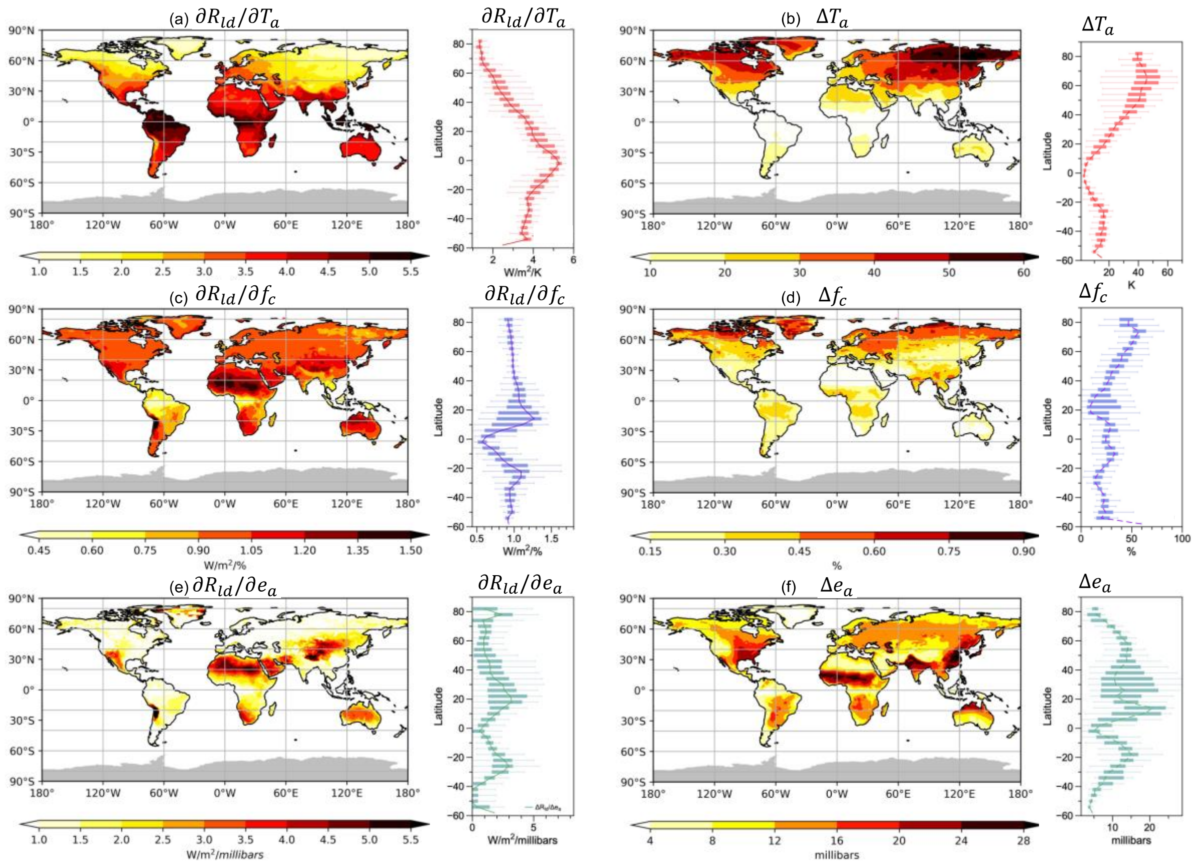

Figure S8. Distribution of the sensitivity of the seasonal cycle of R_{ld} to (a) surface air temperature ($\frac{\partial R_{ld}}{\partial T} = 4\sigma\bar{\varepsilon}\overline{T_a}^3$), (c) cloud cover ($\frac{\partial R_{ld}}{\partial f_c} = \sigma\overline{T_a}^4 \times \left(1 - 1.24\left(\frac{\overline{e_a}}{\overline{T_a}}\right)^{\frac{1}{7}}\right)$), (e) and water vapor pressure ($\frac{\partial R_{ld}}{\partial e_a} = \sigma\overline{T_a}^4 \times \frac{1.24}{7}\frac{(1-\overline{f_c})}{(\overline{e_a})^{\frac{6}{7}}(\overline{T_a})^{\frac{1}{7}}}$), and their latitudinal variations. Distribution of the seasonal cycle of (b) surface air temperature, (d) cloud cover, and (f) water vapor pressure, and their latitudinal variations. Seasonal cycle (Δ) indicates the difference between the maximum and minimum monthly data. In maps, grey shading indicate missing values. In boxplots, the box shows the variation among the land grids at the same latitude, while the solid line is their mean. The upper and lower whisker indicate 95th and 5th percentiles, upper boundary, median line, and lower boundary of the box indicate the 75th, 50th, 25th quantiles, respectively. Data are from the NASA-CERES dataset.

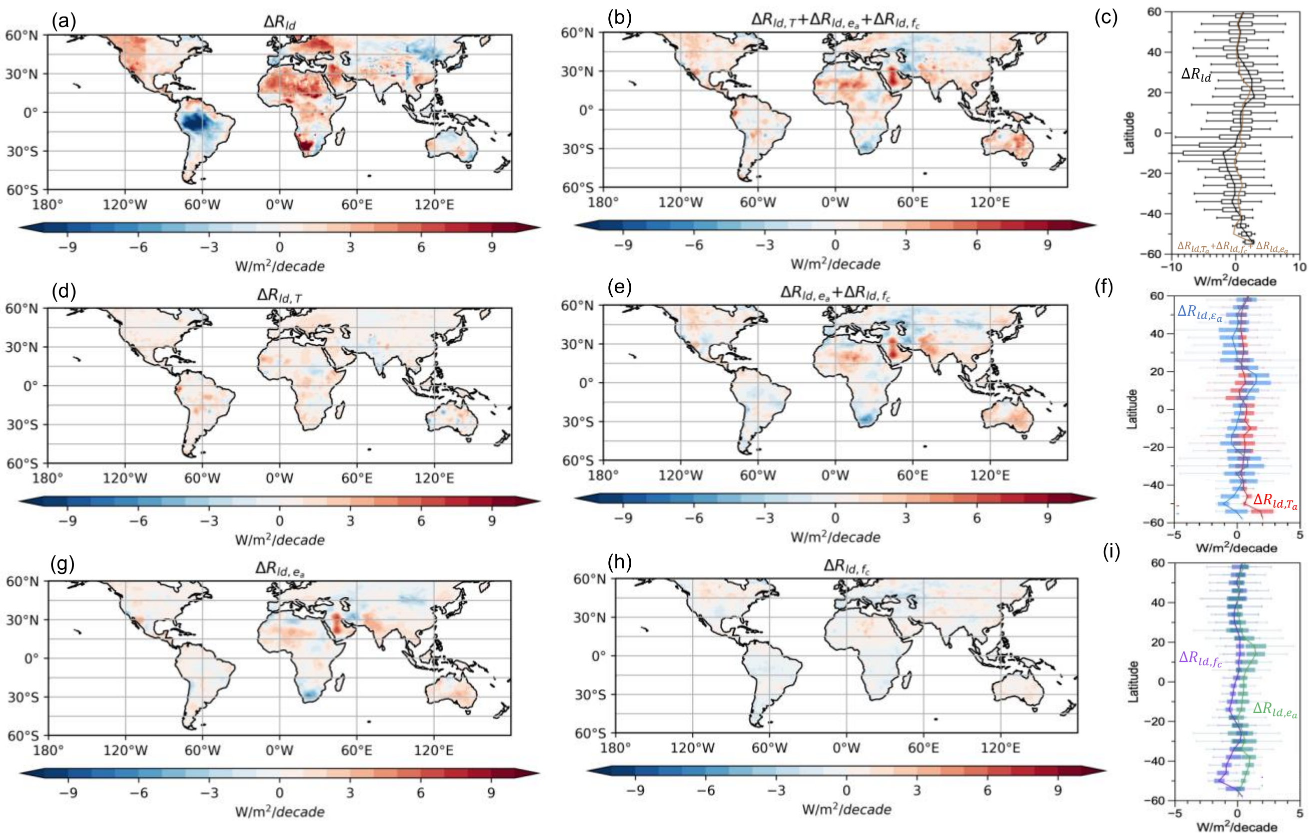

Figure S9. Decomposition of the interannual trend of R_{ld} (ΔR_{ld}) (a) to the interannual trend of surface air temperature ($\Delta R_{ld,T} = 4\bar{\varepsilon}\sigma\overline{T_a}^3\Delta T_a$) (d) and emissivity ($\Delta R_{ld,e_a} + \Delta R_{ld,f_c}$) (e), which composites of contributions of water vapor pressure ($\Delta R_{ld,e_a} = \sigma\overline{T_a}^4 \times \frac{1.24}{7}\frac{(1-\overline{f_c})}{(\overline{e_a})^{\frac{6}{7}}(\overline{T_a})^{\frac{1}{7}}})\Delta e_a$) (g) and cloud cover ($\Delta R_{ld,f_c} = \sigma\overline{T_a}^4 \times \left(1 - 1.24\left(\frac{\overline{e_a}}{\overline{T_a}}\right)^{\frac{1}{7}}\right)\Delta f_c$) (h), and their sum ($\Delta R_{ld,T} + \Delta R_{ld,e_a} + \Delta R_{ld,f_c}$) (b). Figs. c, f, and i show the corresponding latitudinal variations. $\overline{\ }$ denotes the multi-year average, and Δ denotes the slope of linear-regression of the yealy-mean data. In Figs. a, b, d,e, g, and h, grey shading indicate missing values. In Figs. c, f, and i, the box shows the variation among the land grids at the same latitude, while the solid line is their mean. The upper and lower whisker indicate 95th and 5th percentiles, upper boundary, median line, and lower boundary of the box indicate the 75th, 50th, 25th quantiles, respectively. Data are from the NASA-CERES dataset.